Effect of Diffusional Limitations on the Gelation of Cyanate Ester Resins

YONG DENG, GEORGE C. MARTIN

Department of Chemical Engineering and Materials Science, Syracuse University, Syracuse, New York 13244

Received 6 March 1996; accepted 12 June 1996

ABSTRACT: The effect of diffusion control-induced unequal reactivities of functional groups on the gelation of cyanate ester resins was analyzed. By introducing differentiation into the recursive approach, a gelation model was developed to calculate the gel points of systems under diffusional limitations. Modeling results for a Zn-catalyzed cyanate resin show that the unequal reactivities have a significant effect on the gel point and the gelation is delayed to a higher conversion. However, other factors, which may include localized reactions and cycle formation, also contribute to the delay of gelation. © 1997 John Wiley & Sons, Inc. J Appl Polym Sci **64:** 115–125, 1997

Key words: Gelation; diffusion control; cyanate ester resins

INTRODUCTION

Gelation of a thermoset occurs at a particular point during cure when an infinite and insoluble molecular network is formed. The 3-dimensional network may be considered as a new phase compared to the individual or free polymer chains in the system although there is no phase boundary between the network and the free chains. The transition point, or the gel point, is defined unambiguously by the instant at which the weight-average molecular weight diverges to infinity. Upon gelation, macroscopic flow becomes impossible and stress relaxation is difficult. Thus, from a processing point of view, it is very important to know the exact gel point.

The ideal case of gelation has been solved by the mean-field theory and conforms to three assumptions, i.e., equal reactivity of functional groups of the same type, independence of reactions, and no cycle formation in the solubles.[1] Flory[1] introduced the concept of a branching coefficient in order to calculate the gel point, whereas the approach of probability generating functions[2] and the recursive approach[3] directly evaluate the weight-average molecular weight. The recursive approach is easy to use and has been employed to deal with cases with nonrandom reactions, including unequal reactivities,[4] substitution effects,[5] and living polymerization.[6]

Cyanate ester resins are thermosetting, high-performance resins, which are considered especially suitable for composite and electronic applications. During commercial processing, the resins are often catalyzed with coordination metals, such as Zn and Mn, and the reaction kinetics has been found to become diffusion-controlled prior to gelation.[7–10] The gelation of the resins has been reported to occur at a conversion higher than the prediction of the mean-field theory,[7,8,11] which is considered as being related to the diffusion control.[8]

Diffusion control is expected to affect gelation in the following two ways: One is due to the localization of reactions and cycle formation resulting from reduced chain mobilities. The other is due to the chain length-dependent reactivities or the unequal reactivities among chains of different sizes. Because of diffusional limitations, functional groups in two chains of unequal sizes pos-

Correspondence to: G. C. Martin.

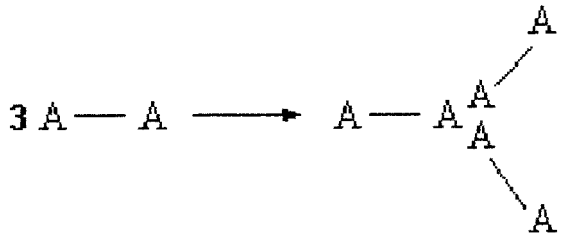

Figure 1 A_2 trimerization reaction.

sess unequal diffusivities and reactivities and, more importantly, the ratio of the two reactivities varies with the changing diffusivities instead of remaining constant as in the case described in Ref. 4.

Sarmoria et al.[12] studied a linear polymerization system with intramolecular reactions or cycle formation. Gupta et al.[11] examined the effect of diffusion on A_f-homopolymerization using a percolation approach. By considering the probability of a reaction being dependent on the distance between reactants, the effect of localized reactions was examined, whereas the effect of chain-length-dependent reactivities was ignored. It was found that the cycle formation is only partially responsible for the delay of gelation and significant contributions are also due to the restriction of the reactions to the neighborhood of the reactants. Such an approach does not require the use of the diffusion coefficient of the polymer chains.

Recently, a modeling strategy was developed for estimating the average diffusion coefficient of polymers during cure[13] and was utilized to study the diffusion phenomena of a zinc-catalyzed cyanate ester resin.[9,10] This made it possible to examine directly the effect of the cure-dependent diffusivity in the system.

The objective of the present work was to analyze the effect of diffusion-induced chain-length-dependent reactivities on the gelation of cyanate ester resins to determine the various contributions to the delay of gelation. Differentiation is introduced into the recursive approach to derive a gelation model by neglecting localized reactions and cycle formation. The model predictions are compared to the experimental gelation data for the zinc-catalyzed cyanate ester resin system.

GELATION MODEL

Consider an A_2-trimerization (A represents a cyanate group) with no cycle formation or localized reactions as shown in Figure 1. Under diffusional limitations, the functional groups may have a great number of reactivities and the reactions are nonrandom. Because the ratio of the reactivities varies constantly, the same type of species, e.g., a pentamer, formed at different times should be separately considered in statistical modeling, i.e., they are different "superspecies" as defined in Ref. 6.

To simplify the problem, one can include only two different reactivities at any instant of time by partitioning the pregel system into two parts, one with lower and the other with higher average molecular weights. The unreacted A functional groups in either part are assumed to be equally reactive, but, at any instant of time, those in the low molecular weight (low-MW) part have higher reactivities than those in the high molecular weight (high-MW) part. Over a time increment, during which the ratio of the two reactivities is considered as a constant, new triazines are formed and the exact amount formed may be calculated based on the diffusion-controlled reaction kinetics. The weight-average molecular weight at the end of the increment may be determined using the recursive approach and the system is repartitioned to allow calculations for the next increment. In this way, the weight-average molecular weight at any instant of time may be evaluated and the system gels when the weight-average molecular weight diverges.

Suppose that, at any extent of reaction p, the number- and weight-average molecular weights of the system are $\bar{M}_n$ and $\bar{M}_w$. The corresponding number- and weight-average degrees of polymerization are $\bar{x}_n$ and $\bar{x}_w$ defined by

$$\overline{x_n} = \frac{\sum n_i(2i+1)}{\sum n_i}, \qquad \overline{x_w} = \frac{\sum n_i(2i+1)^2}{\sum n_i(2i+1)} \quad (1)$$

where n_i is the number of chains in the system consisting of $(2i+1)$ A_2-monomer groups or i triazines. All the summations are from $i = 0$ to ∞.

To partition the system, the *unreacted A* groups in the low-MW part are designated by L, and those in the high-MW part, by H. The partition is characterized by three parameters, ρ_0, ρ_1, and ρ_2:

$$\rho_0 = \frac{\sum n_{Li}}{\sum n_i}, \qquad \rho_1 = \frac{\sum n_{Li}(2i+1)}{\sum n_i(2i+1)},$$

$$\rho_2 = \frac{\sum n_{Li}(2i+1)^2}{\sum n_i(2i+1)^2} \quad (2)$$

where n_{Li} is the number of $(2i + 1)$-mers in the low-MW part and n_{Hi} is the number of $(2i + 1)$-mers in the high-MW part. Note that the exact molecular size distribution is unknown and the procedure to perform the partition will be discussed later.

Now, the A_2-trimerization system has been redefined as an L_i–H_i copolymerization system, in which L-bearing molecules can have various molecular weights and a various number of L groups and, similarly, H-bearing molecules can have various molecular weights and various numbers of H groups. Such a system is similar to the A_{fi}–B_{gi} copolymerization system discussed by Macosko and Miller[3] except that L/H groups may also react among themselves. Note that, immediately after each partitioning, the newly defined L–H system does not contain any reacted L or H groups. Following the partitioning, reactions occur and the L and the H groups react to form new triazines.

The recursive approach may be used to evaluate the weight-average molecular weight over a time increment Δt. Let Δq_1 be the fraction of A groups that belong to the new LLL triazines (those with three L groups) formed within Δt. Δq_2, Δq_3, and Δq_4 are similarly defined for those fractions of A groups that belong to LLH, LHH, and HHH triazines, respectively. Their values may be determined based on the reaction kinetics.

Since a chain consisting of i triazines has $(i + 2)$ unreacted A groups, the total number of L groups in the system is

$$\sum n_{Li}(i + 2) = \tfrac{1}{2}\sum n_{Li}(2i + 1) + \tfrac{3}{2}\sum n_{Li} = \tfrac{1}{2}\rho_1 \sum n_i(2i + 1) + \tfrac{3}{2}\rho_0 \sum n_i \quad (3)$$

The number of H groups in the system may be similarly obtained.

Because there are two L groups and one H group in an LLH triazine, the probability that a randomly selected L is reacted and is part of an LLH triazine (note that the latter statement also means L is reacted) is simply the number of such L groups divided by the number of L groups in the system:

$$\frac{2\sum n_i(2i + 1)\cdot\frac{2}{3}\Delta q_2}{\frac{1}{2}\rho_1 \sum n_i(2i + 1) + \frac{3}{2}\rho_0 \sum n_i} = \frac{4\overline{x_n}}{\rho_1\overline{x_n} + 3\rho_0}\frac{2}{3}\Delta q_2 \quad (4)$$

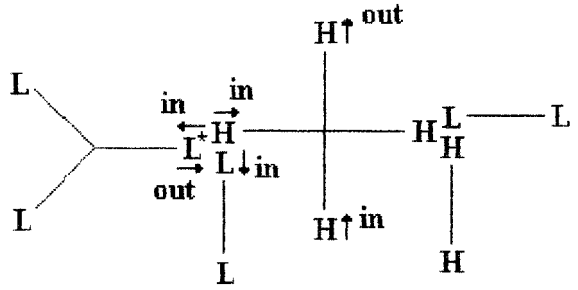

Figure 2 A cyanate chain with *LLH* and *LHH* triazines.

Note that $2\sum n_i(2i + 1)$ is the total number of A groups in the system. Similar probabilities may also be obtained for L and H as parts of other types of new triazines. Next, the expected weights are evaluated following the procedure given in Ref. 3 for A_{fi}–B_{gi} copolymerization.

For a randomly selected L, the expected weight attached if looking out from L (see Fig. 2), $E(W_L^{\text{out}})$, depends on whether L is reacted or not. If L is unreacted, the expected weight is zero. If L belongs to an LLH triazine, e.g., L^* in Figure 2, the expected weight is the probability that L belongs to an LLH triazine, given by eq. (4), multiplied by the sum of the expected weight attached if looking into a randomly selected L, $\sum E(W_{Li}^{in})l_i$, and that if looking into a randomly selected H, $\sum E(W_{Hi}^{in})h_i$. Since an L group may also belong to other types of triazines, then

$$E(W_L^{out}) = \frac{4\overline{x_n}}{\rho_1\overline{x_n} + 3\rho_0}\left\{\Delta q_1 2\sum E(W_{Li}^{in})l_i + \frac{2}{3}\Delta q_2\left[\sum E(W_{Li}^{in})l_i + \sum E(W_{Hi}^{in})h_i\right] + \frac{1}{3}\Delta q_3 2\sum E(W_{Hi}^{in})h_i\right\} \quad (5)$$

where $E(W_{Li}^{in})$ is the expected weight looking into a randomly selected L_i molecule (an L_i is a molecule in the low-MW part that has i triazines and l_i is the mol fraction of L groups in all of the L_i molecules; H_i and h_i are similarly defined).

Also,

$$E(W_H^{out}) = \frac{4\overline{x_n}}{(1-\rho_1)\overline{x_n} + 3(1-\rho_0)} \times \left\{ \Delta q_4 2 \sum E(W_{Hi}^{in}) h_i + \frac{2}{3}\Delta q_3 \left[\sum E(W_{Li}^{in}) l_i + \sum E(W_{Hi}^{in}) h_i \right] + \frac{1}{3}\Delta q_2 2 \sum E(W_{Li}^{in}) l_i \right\} \quad (6)$$

Since there are $(2i+1)A_2$ monomer groups or $(i+2)L$ (unreacted A) groups in an L_i molecule, one can easily find that

$$E(W_{Li}^{in}) = M_{A_2}(2i+1) + (i+1)E(W_L^{out}) \quad (7)$$

and

$$E(W_{Hi}^{in}) = M_{A_2}(2i+1) + (i+1)E(W_H^{out}) \quad (8)$$

$$l_i = \frac{n_{Li}(i+2)}{\sum n_{Li}(i+2)}, \quad h_i = \frac{n_{Hi}(i+2)}{\sum n_{Hi}(i+2)} \quad (9)$$

Thus, after simplification,

$$\sum E(W_{Li}^{in}) l_i = \frac{(2\overline{x_{wL}}\overline{x_{nL}} + 6\overline{x_{nL}})M_{A_2} + (\overline{x_{wL}}\overline{x_{nL}} + 4\overline{x_{nL}} + 3)E(W_L^{out})}{2\overline{x_{nL}} + 6} \quad (10)$$

$$\sum E(W_{Hi}^{in}) h_i = \frac{(2\overline{x_{wH}}\overline{x_{nH}} + 6\overline{x_{nH}})M_{A_2} + (\overline{x_{wH}}\overline{x_{nH}} + 4\overline{x_{nH}} + 3)E(W_H^{out})}{2\overline{x_{nH}} + 6} \quad (11)$$

where the degrees of polymerization are all determined by the partition

$$\overline{x_{nL}} = \frac{\rho_1}{\rho_0}\overline{x_n}, \ \overline{x_{nH}} = \frac{(1-\rho_1)}{(1-\rho_0)}\overline{x_n}, \quad \overline{x_{wL}} = \frac{\rho_2}{\rho_1}\overline{x_w}, \ \overline{x_{wH}} = \frac{(1-\rho_2)}{(1-\rho_1)}\overline{x_w} \quad (12)$$

Substituting eqs. (10) and (11) into eqs. (5) and (6) yields

$$E(W_L^{out}) = \frac{4\overline{x_n}}{\rho_1\overline{x_n} + 3\rho_0} \left[\left(2\Delta q_1 + \frac{2}{3}\Delta q_2 \right) \times \frac{\overline{x_{wL}}\overline{x_{nL}} + 4\overline{x_{nL}} + 3}{2\overline{x_{nL}} + 6} E(W_L^{out}) + \left(\frac{2}{3}\Delta q_2 + \frac{2}{3}\Delta q_3 \right) \frac{\overline{x_{wH}}\overline{x_{nH}} + 4\overline{x_{nH}} + 3}{2\overline{x_{nH}} + 6} \times E(W_H^{out}) + \left(2\Delta q_1 + \frac{2}{3}\Delta q_2 \right) \frac{2\overline{x_{wL}}\overline{x_{nL}} + 6\overline{x_{nL}}}{2\overline{x_{nL}} + 6} \times M_{A_2} + \left(\frac{2}{3}\Delta q_2 + \frac{2}{3}\Delta q_3 \right) \frac{2\overline{x_{wH}}\overline{x_{nH}} + 6\overline{x_{nH}}}{2\overline{x_{nH}} + 6} M_{A_2} \quad (13)$$

and

$$E(W_H^{out}) = \frac{4\overline{x_n}}{(1-\rho_1)\overline{x_n} + 3(1-\rho_0)} \times \left[\left(2\Delta q_4 + \frac{2}{3}\Delta q_3 \right) \frac{\overline{x_{wH}}\overline{x_{nH}} + 4\overline{x_{nH}} + 3}{2\overline{x_{nH}} + 6} \times E(W_H^{out}) + \left(\frac{2}{3}\Delta q_2 + \frac{2}{3}\Delta q_3 \right) \times \frac{\overline{x_{wL}}\overline{x_{nL}} + 4\overline{x_{nL}} + 3}{2\overline{x_{nL}} + 6} \times E(W_L^{out}) + \left(2\Delta q_4 + \frac{2}{3}\Delta q_3 \right) \times \frac{2\overline{x_{wH}}\overline{x_{nH}} + 6\overline{x_{nH}}}{2\overline{x_{nH}} + 6} \times M_{A_2} + \left(\frac{2}{3}\Delta q_2 + \frac{2}{3}\Delta q_3 \right) \frac{2\overline{x_{wL}}\overline{x_{nL}} + 6\overline{x_{nL}}}{2\overline{x_{nL}} + 6} M_{A_2} \quad (14)$$

Consequently, $E(W_L^{out})$ and $E(W_H^{out})$ may be written as functions of the other variables in eqs. (13) and (14) by solving the two equations simultaneously. The expected weight of picking an L_i or H_i can also be found since

$$E(W_{Li}) = E(W_{Li}^{in}) + E(W_L^{out}) = (2i + 1)M_{A_2} + (i + 2)E(W_L^{out})$$
$$E(W_{Hi}) = E(W_{Hi}^{in}) + E(W_H^{out}) = (2i + 1)M_{A_2} + (i + 2)E(W_H^{out}) \quad (15)$$

Then, the weight-average molecular weight $\bar{M}_w$ may be evaluated by randomly picking a unit of mass and calculating the expected weight of the molecule to which it belongs:

$$\overline{M_w} = \sum w_{Li}E(W_{Li}) + \sum w_{Hi}E(W_{Hi}) \quad (16)$$

where the weight fractions are defined by

$$w_{Li} = \frac{n_{Li}(2i+1)}{\sum n_i(2i+1)}, \qquad w_{Hi} = \frac{n_{Hi}(2i+1)}{\sum n_i(2i+1)} \quad (17)$$

Finally, by subtracting the value of $\bar{M}_w$ at the beginning of the time increment, one obtains

$$\Delta\overline{M_w} = \tfrac{1}{2}E(W_L^{out})(\rho_2\overline{x_w} + 3\rho_1) + \tfrac{1}{2}E(W_H^{out})[(1 - \rho_2)\overline{x_w} + 3(1 - \rho_1)] \quad (18)$$

This is the increment in $\bar{M}_w$ over the time increment Δt. $E(W_L^{out})$ and $E(W_H^{out})$ are found by solving two linear algebraic equations, eqs. (13) and (14). The other quantities in eqs. (13), (14), and (18) are determined by the partition and the reaction kinetics. The weight-average molecular weight at any instant of time may be evaluated by solving eq. (18), equivalent of a differential equation.

Equation (18) is the gelation model and is an exact solution for A_2-trimerization with no cycle formation. Modeling errors may, however, arise from errors in the modeling of the reaction kinetics and in the partitioning of the cure system.

ANALYSIS OF A Zn-CATALYZED CYANATE SYSTEM

The cure-dependent diffusion and the diffusion-controlled kinetics of a bisphenol A dicyanate (BADCy)/100 ppm Zn resin system have recently been studied.[9,10] The normalized diffusion coefficient, the average diffusivity of the polymers normalized with respect to its value at 25% conversion, during isothermal cure at temperatures between 130 and 170°C was evaluated based on dielectric monitoring of the curing. At the early stage of cure, the reaction follows a second-order rate law, while under the diffusion-controlled regime, it may be well described by the following kinetic model:

$$\frac{d\alpha}{dt} = k(1 - \alpha)^2 = \frac{k_p k'_{d0}\dfrac{D}{D_{\alpha=0.25}}}{k_p + k'_{d0}\dfrac{D}{D_{\alpha=0.25}}}(1 - \alpha)^2 \quad (19)$$

where α is the cyanate conversion; k, the apparent rate constant and approximately equal to k_p at very low conversions; k_p, the intrinsic rate constant or the rate constant of the second-order rate law; k'_{d0}, a constant at isothermal conditions; $D/D_{\alpha=0.25}$, the normalized diffusion coefficient; and t, time. The results, including the kinetic data measured with Fourier transform infrared spectroscopy, of this study were used in the present work.

Various experimental methods exist for detecting the gel point of a thermoset. For example, the gel point may be found by extrapolating the data for the weight fraction of solubles to one,[14,15] by extrapolating the steady shear viscosity to infinity,[14,16,17] and by the storage and loss moduli crossover method.[15,18,19] Owusu[8] studied the gelation of BADCy catalyzed by Zn, Mn, and Co catalysts with or without an OH cocatalyst and found that the gel points measured using the weight fraction of solubles, the steady shear viscosity, and the moduli crossover are in agreement.

The moduli crossover method was used to determine the gel point of the BADCy/Zn resin system. In conducting the dynamic mechanical analysis, a Bohlin rheometer system was utilized to monitor the storage and loss moduli of a sample under isothermal cure. During each test, the sample was placed between a pair of heated parallel plates (size: 2.54 cm in diameter; gap: 0.159 cm). As the resin curing proceeded, sinusoidal oscillations of 1 Hz with a strain amplitude of 1% were applied to one plate and the stress and phase angle of the other plate were recorded. Based on the experimental data, the dynamic moduli were evaluated. Figure 3 shows the storage modulus, G', and the loss modulus, G''. The gel time was taken as the time at which G' equals G''.

As mentioned earlier, the overall curing reac-

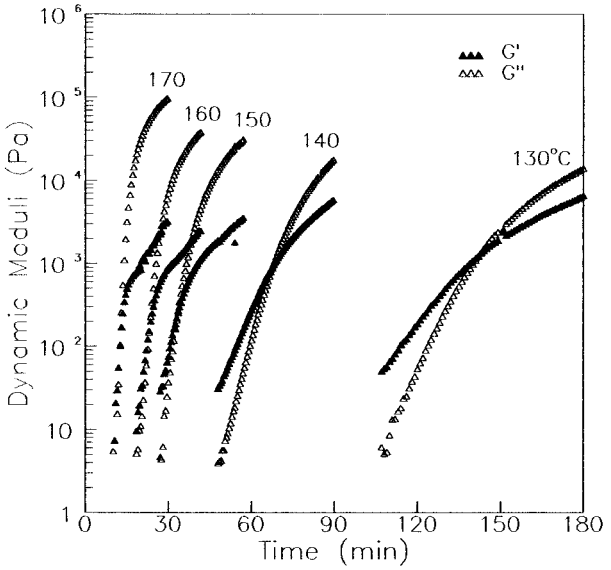

Figure 3 Storage and loss moduli at 1 Hz.

tion appears to be second order. Yet, a triazine is formed by three cyanate groups. What is the rate equation for cyanates with unequal reactivities? To derive such an equation, it is noted that a significant number of dimers was not detected in size exclusion chromatography analysis of the BADCy/Zn system.[10] Hence, the addition of a third cyanate to a dimer may be considered as very fast or zero order. If each of the first two cyanates constitutes one order in the reaction kinetics, the overall reaction is second order. Thus, for triazines formed by cyanates of unequal reactivities, the rate equation may be written as

$$r_c = kc_1c_2\frac{c_3}{c} \tag{20}$$

where r_c is the rate of triazine formation; c, the concentration of all the cyanates; and c_1, c_2, and c_3, the concentrations of cyanates with different reactivities. This equation reduces to the second-order rate law if all the cyanates are equally reactive and is valid for the reaction schemes proposed by both Bauer et al.[20] and Simon and Gillham,[21] which involve the formation of imidocarbonate. Equation (20) was used in the gelation modeling to determine the rates of formation, Δq_1, Δq_2, Δq_3, and Δq_4, of the four types of triazines.

For the formation of *LLL* and *HHH* triazines, D_L (diffusion coefficient of chains in the low-MW part) and D_H (diffusion coefficient of chains in the high-MW part) were used as the corresponding diffusion coefficients. For *LLH* triazines, the slowest step is the *L*–*H* reaction. Hence, the diffusion coefficient was chosen as $(D_L + D_H)/2$. Similarly, for *LHH* triazines, the diffusion coefficient was D_H. Thus, the four rate coefficients are

$$k_1 = \frac{k_p k'_{d0}\dfrac{D_L}{D_{\alpha=0.25}}}{k_p + k'_{d0}\dfrac{D_L}{D_{\alpha=0.25}}},$$

$$k_4 = \frac{k_p k'_{d0}\dfrac{D_H}{D_{\alpha=0.25}}}{k_p + k'_{d0}\dfrac{D_H}{D_{\alpha=0.25}}} \tag{21}$$

where k_1, k_2, k_3, and k_4 are the rate coefficients for the formation of *LLL*, *LLH*, *LHH*, and *HHH* triazines, respectively, and the normalized diffusion coefficients are given by

$$k_2 = \frac{k_c k'_{d0}\dfrac{D_L + D_H}{2D_{\alpha=0.25}}}{k_c + k'_{d0}\dfrac{D_L + D_H}{2D_{\alpha=0.25}}}, \quad k_3 = k_4$$

$$\frac{D_L}{D_{\alpha=0.25}} = \frac{D}{D_{\alpha=0.25}}\frac{\overline{x_n}}{\overline{x_{nL}}} = \frac{D}{D_{\alpha=0.25}}\frac{\rho_0}{\rho_1},$$

$$\frac{D_H}{D_{\alpha=0.25}} = \frac{D}{D_{\alpha=0.25}}\frac{1-\rho_0}{1-\rho_1} \tag{22}$$

Since the fractions of *L* and *H* among all the unreacted *A* or cyanates are

$$\frac{\sum n_{Li}(i+2)}{\Sigma n_i(i+2)} = \frac{\rho_1\overline{x_n} + 3\rho_0}{\overline{x_n} + 3},$$

$$\frac{\sum n_{Hi}(i+2)}{\Sigma n_i(i+2)} = \frac{(1-\rho_1)\overline{x_n} + 3(1-\rho_0)}{\overline{x_n} + 3} \tag{23}$$

respectively, Δq_1, Δq_2, Δq_3, and Δq_4 may be written as

$$\Delta q_1 = k_1\left(\frac{\rho_1\overline{x_n} + 3\rho_0}{\overline{x_n} + 3}\right)^3(1-\alpha)^2\Delta t$$

$$\Delta q_2 = k_2\left(\frac{\rho_1\overline{x_n} + 3\rho_0}{\overline{x_n} + 3}\right)^2 \times \frac{(1-\rho_1)\overline{x_n} + 3(1-\rho_0)}{\overline{x_n} + 3}(1-\alpha)^2\Delta t$$

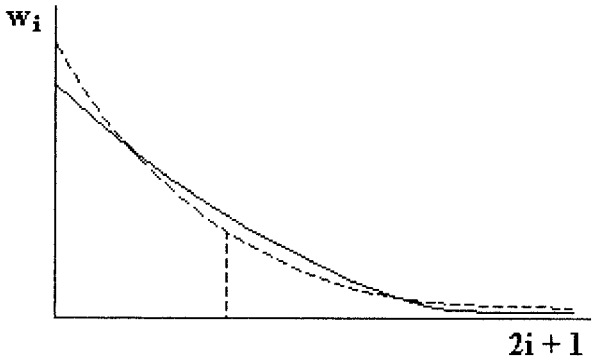

Figure 4 Molecular size distributions of a diffusion-limited system (solid) and its reference system described by the mean-field prediction (dashed).

$$\Delta q_3 = k_3 \frac{\rho_1 \overline{x_n} + 3\rho_0}{\overline{x_n} + 3} \times \left[\frac{(1 - \rho_1)\overline{x_n} + 3(1 - \rho_0)}{\overline{x_n} + 3} \right]^2 (1 - \alpha)^2 \Delta t$$

$$\Delta q_4 = k_4 \left[\frac{(1 - \rho_1)\overline{x_n} + 3(1 - \rho_0)}{\overline{x_n} + 3} \right]^3 (1 - \alpha)^2 \Delta t \quad (24)$$

The rates of triazine formation so obtained were then scaled with respect to the overall rate of reaction so that the sum of the four rates used in the modeling is equal to the overall rate of reaction since only the relative values of the four rates are important for the gelation modeling.

What has not been discussed above is how the cure system can be partitioned. In principle, there are numerous ways to perform the partition. Among the ideal ones is the chain-length partition. In an ideal chain-length partition, a partition chain length is used as a threshold such that the low-MW part is composed of chains shorter than or equal to the partition chain length and the high-MW part is composed of chains longer than the partition chain length. However, to perform an ideal chain-length partition, it is necessary to know the molecular size distribution, which is not available in the proposed gelation model. An alternative approach is to allow long chains to exist in the low-MW part and vice versa but to ensure that the *average* molecular weight of the low-MW part is lower than that of the high-MW part.

Figure 4 illustrates qualitatively the molecular size distributions (weight fraction w_i vs. chain length) of a diffusion-limited system (solid) and its reference system (dashed). The distribution in the reference system is given by the mean-field prediction[9,10]:

$$w_i = \frac{(2i + 2)!}{(i + 1)!(i + 2)!} p^i (1 - p)^{i+2} \quad (25)$$

The area under either curve is equal to 1 and the two distributions have the same weight-average molecular weight. The dashed vertical line indicates the partition chain length applied to the reference system to obtain parameter ρ_1, which equals the area under the dashed curve on the left of the dashed line.

Under diffusional limitations, a functional group in a short chain is more reactive than is a functional group in a long chain. The diffusion-limited system has smaller weight fractions of short chains and long chains and larger fractions of mid-sized chains. Close to the partition chain length (dashed line), the difference between the diffusion-limited distribution and the mean-field distribution is relatively large, because when short chains react to form chains longer than the partition chain-length, the reactivity and the probability for further growth are reduced.

Performing an ideal chain-length partition on the reference system results in a set of partition parameters, ρ_0, ρ_1, and ρ_2. However, because of the difference in the molecular weight distributions of the diffusion-limited system and the reference system and the fact that ρ_2 places a larger weight on long chains than does ρ_1 by definition, this ρ_2 is too small for the diffusion-limited system (see Ref. 22 for more details). Similarly, this ρ_0 is too large for the diffusion-limited system. The partition described by the three parameters does not exist in the diffusion-limited system and needs to be modified to allow some long chains to stay in the low-MW part and vice versa.

Define a chain-length increment $\delta\phi_L$:

$$\delta\phi_L = \left(\frac{\overline{x_n}}{\overline{x_{nr}}} - 1 \right) \phi_L \quad (26)$$

where ϕ_L is the partition chain length and subscript r indicates the corresponding reference system. Using number-averaged molecular weight has the advantage that it exists even after gelation. Because the weight-average molecular weight of a cure system under diffusional limitations is always smaller than or equal to that of an equal-reactivity system of the same degree of conver-

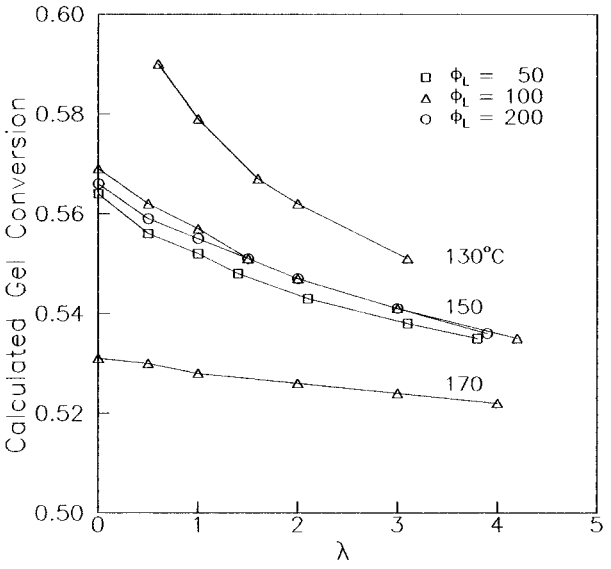

Figure 5 Calculated gel conversion vs. constant λ.

sion, $\bar{x}_n$ of the diffusion-limited system is always larger than or equal to $\bar{x}_{nr}$ of the corresponding reference system, which has the same weight-average molecular weight. An ideal chain-length partition may then be performed on the reference system using partition chain-length ϕ_L to obtain ρ_1, which are followed by two more ideal partitions using $(\phi_L - \lambda\delta\phi_L)$ and $(\phi_L + \lambda\delta\phi_L)$ as partition chain lengths to obtain ρ_0 and ρ_2 (λ is a constant and is larger than or equal to 0), respectively. The value of λ determines the degree of modifications to the partition using a single partition chain length. If λ is very small, the partition may not exist in the diffusion-limited system. If λ is very large, however, the low-MW part will be composed of many long chains and the high-MW part will be composed of many short chains, making the partition itself less meaningful.

Figure 5 is a plot of the calculated gel conversion vs. the parameter λ. When modeling the gelation of the BADCy/Zn system, two ordinary differential equations, the diffusion-controlled kinetic model [Eq. (19)] and the gelation model $d\bar{M}_w/dt$ derived from Eq. (18), were solved simultaneously using numerical methods. The rate constants, k_c and k'_{d0}, and the normalized diffusion coefficient, $D/D_{\alpha=0.25}$, used in the modeling were those given in Ref. 10. The degree of cyanate conversion whenever the calculated $\bar{M}_w$ exceeded 3×10^7 (an arbitrarily chosen, large number) was taken as the calculated gel conversion of the system. The model was also tested using an unusually large value of k'_{d0} to ensure that the results agreed with the 50% gel conversion predicted by the mean-field theory.

In Figure 5, as λ increases, the calculated gel conversion decreases. When λ is very small, for instance when λ equals zero, the set of partition parameters obtained from the reference system does not exist in the cure system, i.e., ρ_2 is too small and ρ_0 is too large. According to Eq. (22), the calculated D_L is then too large and D_H is too small. Consequently, the difference between the reactivity of short chains and that of long chains is exaggerated, resulting in a relatively high gel conversion. When λ is very large, there are many long chains in the low-MW part and many short chains in the high-MW part. As a result, the calculated gel conversion is low.

During the gelation modeling, the actual modification to the partition chain length, $(\lambda\delta\phi_L)$, is not a constant. Instead, it varies with cure time. When, because of diffusion control, the molecular size distribution of the cure system deviates significantly from that of the corresponding reference system, the modification is large. Otherwise, it is small. Table I shows the maximum modifications, $(\lambda\delta\phi_L)_{max}$, for various values of λ when $\phi_L = 100$ is used. At a low temperature, the effect of diffusion on the reaction kinetics is strong and $(\lambda\delta\phi_L)_{max}$ is large. At a high temperature, $(\lambda\delta\phi_L)_{max}$ is small. When $\lambda = 1$, $(\lambda\delta\phi_L)_{max}$ ranges from 14 to 48% of ϕ_L. When $\lambda = 3$, $(\lambda\delta\phi_L)_{max}$ is as large as 78% of ϕ_L at 130°C and the modification is considered as more than necessary. From $\lambda = 1$ to $\lambda = 3$, the calculated gel conversions decrease by only 0.3–2.5% conversion (Fig. 5), which is relatively small compared to the range of $(\lambda\delta\phi_L)_{max}$. Since a very small λ may result in partitions that do not exist, $\lambda = 1$ was chosen for the present resin system.

Figure 6 shows the dependence of the calculated gel conversion on the partition chain length for the BADCy/Zn system. As one may expect, when ϕ_L is very small or very large, the majority of the molecular species are assigned with the same diffusivity and the same reactivity, resulting in virtually meaningless partitions and relatively low gel conversion. The effect of diffusion on the gel conversion is well described by the model when the partition chain length is adequately selected. In Figure 6, the calculated gel conversion reaches its peak value at a partition chain length between 50 and 300, and the variation of the calculated gel conversion appears to be small compared to the change in the partition chain length. Since the partition of the cure sys-

Table I Maximum Modifications for $\phi_L = 100$

T = 130°C		T = 150°C		T = 170°C	
λ	$(\lambda\delta\phi_L)_{max}$	λ	$(\lambda\delta\phi_L)_{max}$	λ	$(\lambda\delta\phi_L)_{max}$
0.6	36	0.5	18	0.5	8
1.0	48	1.0	30	1.0	14
1.6	60	1.5	40		
2.0	66	2.0	48	2.0	24
3.1	78	3.0	60	3.0	32
		4.2	70	4.0	40

tem into two parts with equal reactivities is an oversimplification for the unequal reactivities induced by diffusional limitations, the peak values of the calculated gel conversion were taken as the gel conversions of the model.

Figure 7 shows the experimental and the model gel conversions. The open triangles represent data obtained from the moduli crossover method and the closed triangles are the modeling results (with λ = 1). The experimental gelation occurs at a conversion higher than the mean-field prediction and does not change significantly as the cure temperature increases. The same has been found earlier in a separate study.[8] The model gel conversion, however, decreases with increasing temperature, which is anticipated since, at a low temperature, the diffusion control begins at a lower conversion than at a high temperature.[10] As diffusion control causes nonrandom reactions of the cyanate groups, gelation is expected to occur at a conversion higher than the mean-field prediction. Thus, the model shows that the diffusion-induced unequal reactivities play an important role in the delay of gelation of the cyanate resin but the effect is dependent on the cure temperature. In addition, as shown in Figure 7, the model predictions are close to the experimental results at low temperatures, while at high temperatures, they are significantly lower than the corresponding experimental data. The difference between the trend of the experimental data and that of the modeling results suggests that using the diffusion-induced unequal reactivities alone is insufficient to explain the delay of gelation of cyanate resins. Other phenomena, which may include localized reactions and cycle formation, are also important

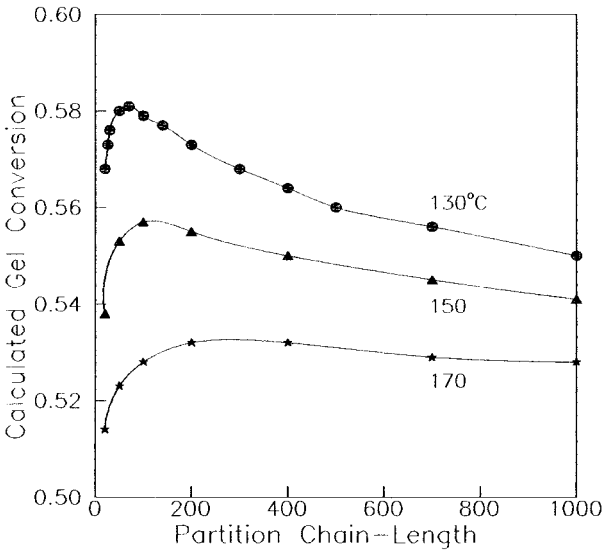

Figure 6 Dependence of calculated gel conversion on partition chain length.

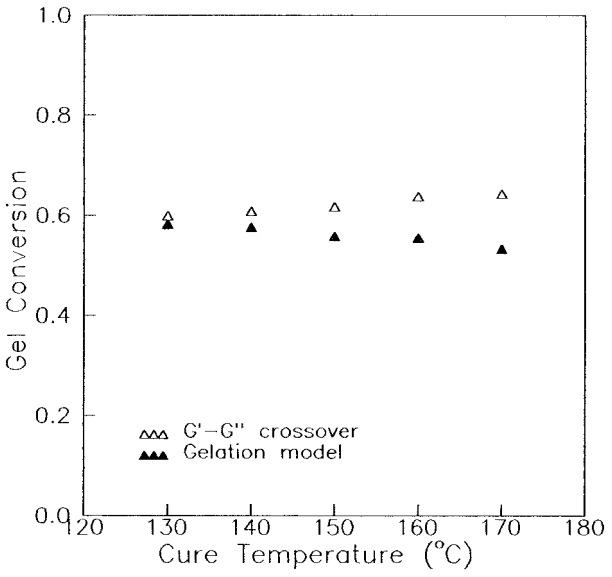

Figure 7 Experimental and model gel conversions for the cyanate resin.

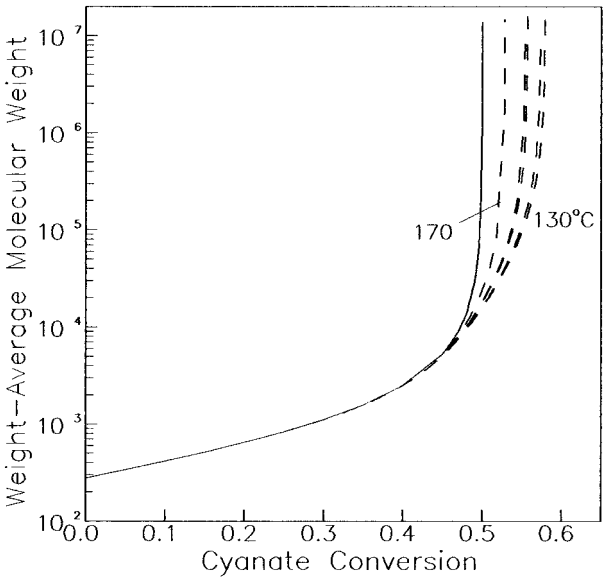

Figure 8 Evolution of the weight-average molecular weight: (——) mean-field prediction; (----) gelation model. From left to right, the corresponding cure temperatures for the dashed curves are 170, 160, 150, 140, and 130°C.

(note that the resin has been assumed, in the present work, to cure through cyclotrimerization; any side reactions, if they exist, will certainly influence the gelation). As it is difficult to incorporate the effect of localized reactions and cycle formation in the recursive approach, some empirical or semiempirical methods may be tested.

Figure 8 illustrates the predicted weight-average molecular weight of the BADCy/Zn resin system. The mean-field prediction indicates that, without diffusional limitations, the weight-average molecular weight remains low up to approximately 40% conversion. After that, $\bar{M}_w$ increases sharply and diverges at 50% conversion. The transition region from low molecular weight to infinity is relatively narrow. However, under diffusional limitations, the weight-average molecular weight predicted by the gelation model starts to deviate from the mean-field prediction at approximately 40% conversion. Although $\bar{M}_w$ also increases sharply close to the gel point, the transition from low molecular weight to infinity occurs over a wider range of conversion because of the diffusional limitations to the formation of long chains. As a result, the gelation is delayed to a higher conversion. The width of the transition region increases with decreasing temperature and the gel conversion is high at a low temperature.

CONCLUSIONS

Diffusional limitations may induce unequal reactivities or chain-length dependence of reactivities among functional groups in a cure system. Due to the changing diffusivities of the molecular species, the ratio of the reactivities varies during cure. By introducing differentiation into the recursive approach, a gelation model was established to take into consideration the effect of the diffusion-induced unequal reactivities on the gelation of cyanate ester resins. This model is an exact solution for the partitioned cure system and predicts the evolution of the weight-average molecular weight.

Modeling results for the BADCy/100 ppm Zn system indicate that the unequal reactivities have a significant effect on the gelation; the transition region for the weight-average molecular weight to evolve from low to infinity is extended and the gelation is delayed to a higher conversion. However, the predicted gel conversion decreases with increasing temperature while the experimental data are largely temperature-independent. This suggests that other factors, which may include localized reactions and cycle formation, are also important in the delay of gelation. The current modeling approach serves as the first step in establishing a comprehensive model for the gelation of cyanate ester resins.

The authors would like to thank G. P. Kohut and J. T. Gotro of IBM for conducting the dynamic mechanical experiments. The highly purified cyanate resin was provided by Ciba-Geigy.

REFERENCES

1. P. J. Flory, *Principles of Polymer Chemistry,* Cornell University Press, Ithaca, NY, 1953.
2. M. Gordon, *Proc. R. Soc. Lond. Ser. A.,* **268,** 240 (1962).
3. C. W. Macosko and D. R. Miller, *Macromolecules,* **9,** 199 (1976).
4. D. R. Miller and C. W. Macosko, *Macromolecules,* **11,** 656 (1978).
5. D. R. Miller and C. W. Macosko, *Macromolecules,* **13,** 1063 (1980).
6. A. M. Gupta and C. W. Macosko, *J. Polym. Sci. Polym. Phys. Ed.,* **28,** 2585 (1990).
7. A. M. Gupta and C. W. Macosko, *Makromol. Chem. Macromol. Symp.,* **45,** 105 (1991).
8. A. O. Owusu, PhD Dissertation, Syracuse University, Syracuse, NY, 1992.

9. Y. Deng and G. C. Martin, *SPE Tech. Pap.,* **40,** 1664 (1994).
10. Y. Deng and G. C. Martin, *Polymer,* **37,** 3593 (1996).
11. A. M. Gupta, R. C. Hendrickson, and C. W. Macosko, *J. Chem. Phys.,* **95,** 2097 (1991).
12. C. Sarmoria, E. M. Vallés, and D. R. Miller, *Macromolecules,* **23,** 580 (1990).
13. Y. Deng and G. C. Martin, *Macromolecules,* **27,** 5141 (1994).
14. S. A. Bidstrup, PhD Dissertation, University of Minnesota, Minneapolis, MN, 1986.
15. H. H. Winter, *Polym. Eng. Sci.,* **27,** 1698 (1987).
16. S. D. Lipshitz and C. W. Macosko, *Polym. Eng. Sci.,* **16,** 803 (1976).
17. A. Apicella, P. Masi, and L. Nicolais, *Rheol. Acta,* **23,** 291 (1984).
18. C. M. Tung and P. J. Dynes, *J. Appl. Polym. Sci.,* **27,** 569 (1982).
19. F. Chambon and H. H. Winter, *Polym. Bull.,* **13,** 499 (1985).
20. M. Bauer, J. Bauer, and G. Kuhn, *Acta Polym.,* **37,** 715 (1986).
21. S. L. Simon and J. K. Gillham, *J. Appl. Polym. Sci.,* **47,** 461 (1993).
22. Y. Deng, PhD Dissertation, Syracuse University, Syracuse, NY, 1994.